

Simulation of crack propagation in rubber

C Timbrell, M. Wiehahn & G. Cook
Zentech International Ltd., Camberley, Surrey, UK

A.H. Muhr
TARRC/Rubber Consultants, Hertford, UK

*Third European Conference On Constitutive Models For Rubber
15-17 September 2003
London, UK*

Full proceedings available in "Constitutive Models for Rubber III", Busfield & Muhr (Eds), Balkema, ISBN 90 5809 566 5

ABSTRACT: Software for simulating crack propagation ("Zencrack") has been developed which handles adaptation of the finite element mesh in the region of the crack tip as the crack propagates, and calls up a finite element solver as a subroutine to calculate the strain energy release rate at each increment in crack length. The objective of this paper is to demonstrate its applicability to rubber components.

First, the reliability of Zencrack, with ABAQUS as the solver, for calculations of strain energy release rate for an edge crack in a strip of rubber in simple extension is investigated. The results are in reasonable agreement with previous analyses and experimental work from the literature. 3D analyses show that the crack front would be expected to develop curvature during propagation. The application of Zencrack to failure of "O" rings by internal cracking is also presented to show how the approach could be applied to a rubber component.

1 INTRODUCTION

The energetics approach, or fracture mechanics, is known to be useful for predicting the fatigue life of rubber components (see for example Gent et al. 1964 and Busfield et al. 1999). However, it calls for the calculation of strain energy release rate, which for the finite strains and complex geometries in typical rubber components necessitates use of large strain Finite Element Analysis (FEA). Unfortunately, such calculations are time-consuming, especially if repetition is required to follow the changes in strain energy release rate as the crack tip advances.

ZENCRACK provides a method for quickly and easily generating 3D finite element models of cracked components. In addition, the mesh is submitted for analysis to a solver such as ABAQUS or MSC.MARC, with subsequent crack growth calculations carried out automatically if required. The crack growth scheme caters for full 3D crack growth of arbitrary 3D crack fronts under mixed mode loading. ZENCRACK is a product of Zentech International Ltd.

In this paper, the capabilities of ZENCRACK for accurate calculation of the strain energy release rate are first investigated, and then the wider issue of its suitability for lifetime prediction is discussed.

2 THEORY

2.1 Energetics approach

Rivlin & Thomas (1953) showed that the fracture of rubber (considered to be perfectly elastic) is controlled by the strain energy release rate, or energy available for tearing, T , defined by:

$$T \equiv -(\partial U / \partial A)_L = -\frac{1}{t} \left(\frac{\partial U_c}{\partial c} \right)_L \quad (1)$$

where the partial derivative indicates that the clamped length L of the testpiece is kept constant so that external forces do no work, U is the total strain energy and the quantities A , c and t are the area of one fracture surface, the crack length and testpiece thickness respectively, referred to the unstrained state. For rubber, we cannot assume strains are infinitesimal, and analytical calculation of T for a particular case may well be intractable. However, Rivlin & Thomas (1953) presented several testpieces for which an analytical expression for T may be derived.

2.2 Linear elastic fracture mechanics

About the same time as Rivlin and Thomas were working on the fracture of rubber, the energetics approach

was also being applied to materials that could only undergo classically small elastic strains, resulting in “linear elastic fracture mechanics” (LEFM). A connection was made for 2D problems between the strain energy release rate and the “stress intensity factor” K_I scaling the stress field in the neighbourhood of the crack tip. Continuing to use the symbol T for the strain energy release rate, this relationship is (eg Ewalds & Wanhill, 1984):

$$T = \frac{K_I^2}{E} \text{ in plane stress} \quad (2)$$

$$T = \frac{K_I^2}{E} (1 - \nu^2) \text{ in plane strain}$$

where E is the Young’s modulus and ν is Poisson’s ratio, the two elastic constants of infinitesimal strain elasticity theory.

Noting that for an incompressible material $\nu = 0.5$ and that $W = \sigma^2 / 2E$ or $3\sigma^2 / 8E$ for a single tensile stress σ in plane stress and plane strain respectively, Equation 2 gives in both cases:

$$T = \frac{2WK_I^2}{\sigma^2} \quad (3)$$

Equation 3 may be used to calculate limiting values of T for infinitesimal strain from published LEFM values of K_I , as given for example in Ewalds & Wanhill (1984). It is perhaps rather surprising that such calculations are believed to yield accurate limiting strain energies, since the LEFM calculations involve a singularity at the crack tip, despite the assumption of infinitesimal strain.

2.3 The J -integral approach for calculation of strain energy release rate

Thomas (1955) went on to show that T , for a crack in a sheet of rubber, may be related to the energy density at the crack tip multiplied by its effective diameter. Rice (1968) built on this approach, showing mathematically that the strain energy release rate, for a 2D infinitesimal strain problem, may be calculated from the stress field by means of a contour integral involving the strain energy density and the tractions and displacements, with the property that any contour, from the free edge on one side of the crack tip to the free edge on the other side, will give the same result. A generalization of Rice’s “ J ”-integral is provided in ABAQUS. It enables the strain energy release rate to be calculated for large strain (Chang 1972) and 3D problems. The latter is addressed by evaluating the integral for a contour in a plane normal to the crack front, and yields a value for the strain energy release rate local to the intersection of the crack front and the plane.

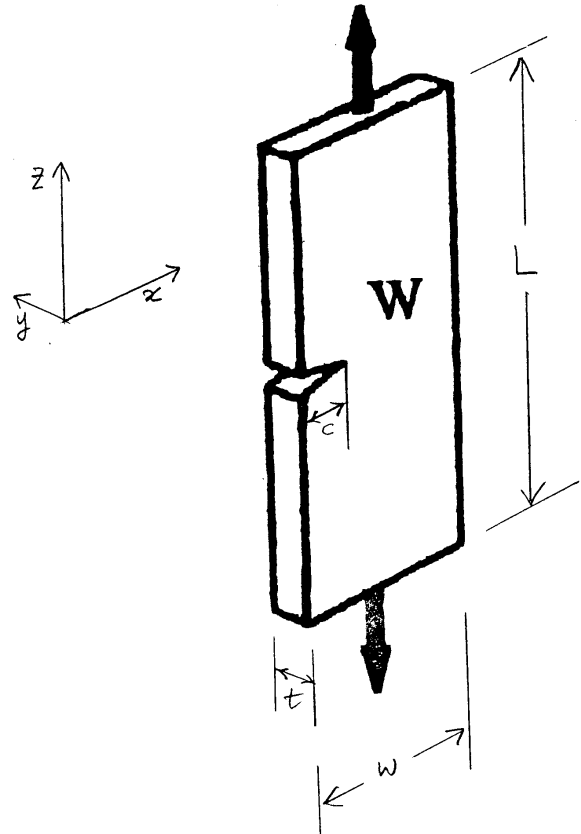


Figure 1. Edge crack in simple extension testpiece

2.4 Edge crack in a simple extension testpiece

Rivlin & Thomas (1953) were also the first to consider a testpiece cut from a sheet of rubber with $t \ll c \ll w \ll L$, where the definition of the symbols is given in Figure 1. c is the length of a small cut in the edge, normal to the direction in which an extension ratio λ is applied.

In the context of fracture tests on other materials, such a testpiece would be referred to as a Single Edge Notch (SEN) testpiece.

Away from the clamps and the cut, the rubber is in a state of uniform simple extension. There will be a complicated region of strain around the cut (but not extending right across the testpiece because $c \ll w$); Rivlin & Thomas (1953) argued that the total elastic energy before (U_0) and after (U_c) the cut c is introduced will obey

$$U_0 - U_c = Kc^2t \quad (4)$$

where K is a constant of proportionality (dependent on strain). The proportionality with c^2 follows from dimensional analysis and the existence of only one length scale associated with the crack, the tip being considered to be ideally sharp. The proportionality with t is valid only if $t \ll c$, so that plane stress conditions prevail over substantially the whole sheet. They further argued that K , a function of λ , may be written as

$$K = kW \quad (5)$$

where W is the strain energy density in the testpiece in the regions of uniform simple extension, and k is a function of λ . In subsequent usage, it has generally been assumed that k is a function only of λ and not of the particular hyperelastic material. In what follows we shall use $(U_0 - U_c)/(Wc^2t)$ for an edge crack as a definition for k , to be used to determine k from experiment, theory or numerical analysis, but we will sometimes discuss also the strain-energy reduction for a crack in the middle of a tensile testpiece

It follows from Equations 1, 4 and 5 that the strain energy release rate T for an edge crack of length c in a tensile testpiece is given by:

$$T = 2kWc \quad (6)$$

Greensmith (1963) pointed out that for infinitesimal strains:

$$k \approx \pi \quad (7)$$

based on the solution for the decrease in strain energy for a crack in the middle of an infinite sheet stretched in the direction normal to the crack orientation (Timoshenko 1934). k will be somewhat greater than π because the plane of symmetry of the crack in the middle of the infinite sheet is not strictly stress free, unlike the free edge for the tensile testpiece with an edge crack. In fact, Ewalds & Wanhill (1983) give a standard solution for the edge crack consistent, for plane stress using Equation 3, with $k = 1.25\pi$.

Greensmith (1963) went on to determine, by experiment, k as a function of λ for four unfilled natural rubber vulcanizates differing in crosslink density. He did this very carefully, measuring the small difference in extension force between a pair of nominally identical testpieces, one with an edge crack and one without, thus increasing the sensitivity and reducing effects of stress relaxation. He found that k was a function only of λ , independent of the particular vulcanizate, and fell from about 3.0 at $\lambda=1$ to about 1.6 at $\lambda=3$.

Lake (1970) derived an approximate formula for k from an estimate of the work required to close a crack in a rubber sheet, based on an analytical argument and measurements of crack opening for testpieces containing central cracks, strained up to 200% or so:

$$k \approx \pi / \sqrt{\lambda} \quad (8)$$

He found this relationship to be a little higher than Greensmith's experimental results over the range $1 < \lambda < 3$ for which he checked it, but nevertheless a useful approximation.

Lindley (1972) carried out further measurements of crack opening, up to 600% strain, and also plane stress finite element analysis of an edge crack. The FEA re-

sults were made at 25% strain for c/w ranging up to 0.3, showing that ΔU is proportional to c^2 for c/w up to about 0.2, and for $c/w = 0.16$ for strains of 5, 10, 50 and 100 and 150%. For the latter strains it was assumed that ΔU is proportional to c^2 . He concluded that his results, and Greensmith's (1963) experimental results were consistent with a somewhat refined version of Equation 8:

$$k \approx \pi(2.95 - 0.08(\lambda - 1)) / \sqrt{\lambda} \quad (9)$$

In all these papers, and in experimental determinations of the crack growth characteristics of rubber compounds (eg Lake & Lindley, 1964) it was assumed that k has no significant dependence on the strain energy function of the rubber.

2.5 Boundary conditions for rubber test pieces, and non-utility of "modes of fracture"

For rubber, the far-field strain needed to make T great enough for studying crack growth in a SEN test piece is typically greater than 10%, and thus variations in nominal strain across the width of the testpiece, caused by imperfect parallelism of the clamps, are of negligible significance. In contrast to the situation with more rigid materials, this means that it is not significant whether the boundary condition at the clamps is uniform stress or uniform displacement.

Large strains also invalidate the principle of superposition of stress-intensity factors for different "modes" of crack propagation, and tend to result in quite different geometries in the strained state than might be anticipated prior to loading. For this reason, the modes of crack propagation used in discussion of fracture of stiff materials are not useful for interpretation of fracture of rubber.

3 FINITE ELEMENT MODELLING OF SEN SPECIMEN

3.1 Geometry

The full model was as shown in Figure 1, with a length, L , of 125mm and a width, w , of 25mm. The thickness, t , and crack length, c , have been varied. A half symmetry model was used for the 2-D analysis, symmetrical about the XY plane. A quarter symmetry Finite Element Model (FEM), symmetrical about the XY and XZ planes, was used for 3-D analyses (see Figure 2). The boundary conditions are such that there are no loads applied in the x and y directions. A common z displacement at the end of the model is used to load the specimen. The units are mm, MPa and Newtons.

An uncracked basic 3-D FEM with four elements through the effective thickness was constructed using

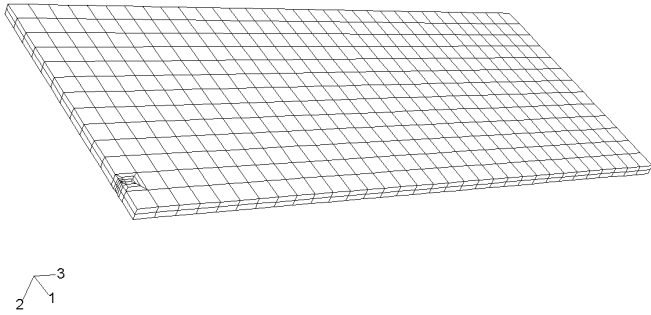


Figure 2. Quarter symmetry 3D FEM; the crack front extends from the front edge along the plane of symmetry at the left hand edge to the centre of the crack block.

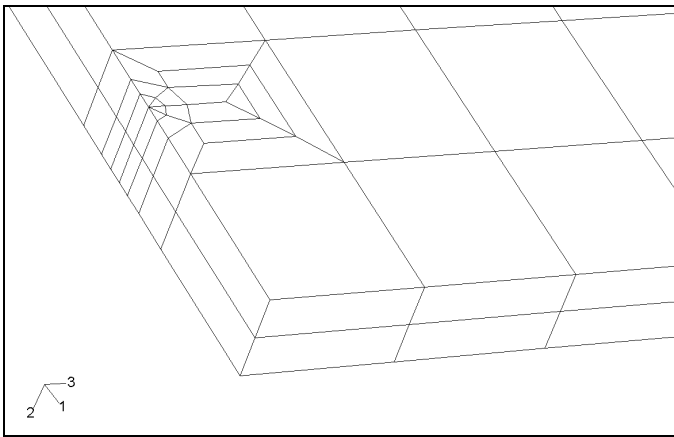


Figure 3. St19x1.sup crack block (half thickness FEM using two crack-blocks)

FEMAP. Zencrack was used to insert the crack into the basic mesh by substituting in a specially meshed “crack block” for part of the FEM (see Figure 2), and to update the boundary conditions as the crack is propagated. The 2-D FEM was constructed from the 3-D FEM using FEMAP.

Three different Zencrack crack blocks have been used in the 3-D analyses containing one, one and five elements respectively through the thickness of the elements of the basic FEM:

- St19x1.sup- A crack block with 19 elements (Figure 3)
- St23x1.sup- A crack block with 23 elements
- St111x5.sup- A crack block with 111 elements (Figure 4).

3.2 Material models

All the material models and their chosen parameters for this report result in incompressible materials. The 3-D models use hybrid elements since the material is fully incompressible. When the material response is incompressible, the solution to a problem cannot be obtained in terms of the displacement history only, since a purely hydrostatic pressure can be added with-

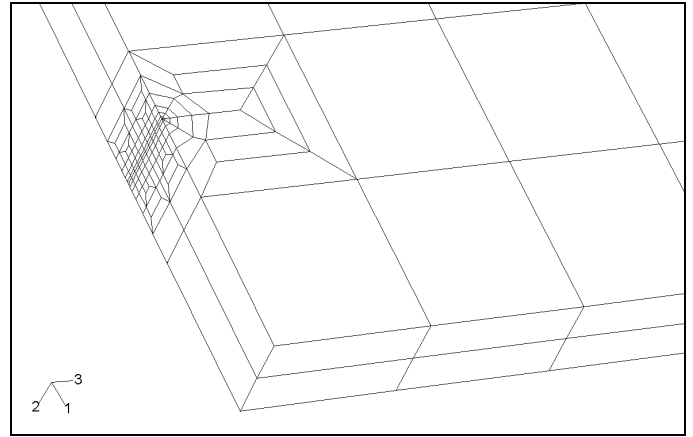


Figure 4. St111x5.sup crack block (half thickness FEM using two crack-blocks)

out changing the displacements. Hybrid elements treat the pressure stress as an independently interpolated basic solution variable and are well suited to incompressible and almost incompressible material behaviour.

When the subroutine UHYPER is used, ABAQUS cannot calculate a default value for the transverse shear stiffness. For continuum elements an hourglass stiffness parameter must be chosen to provide the elements’ transverse shear stiffness and a value of 0.003 was used, this being the default value in the neo-Hookean model pre-programmed into ABAQUS and used for most of the analyses.

To test the independence of k from the choice of strain energy function W , three different models were used:

3.2.1 Neo-Hookean model

This model is pre-programmed into ABAQUS in the form:

$$W = C_{10}(\bar{I}_1 - 3) + \frac{1}{D_1}(J^{el} - 1)^2 \quad (10)$$

where W is the strain energy per unit of reference volume, \bar{I}_1 is the first deviatoric strain invariant, and C_{10} and D_1 are related to the shear modulus G and bulk modulus K by:

$$\begin{aligned} G &= 2C_{10} \\ K &= 2/D_1 \end{aligned} \quad (11)$$

The values used here are $G = 0.5\text{MPa}$, and $D_1 = 0$, representing an incompressible material with a shear modulus typical for an unfilled natural rubber.

3.2.2 Gent model

Gent (1996) published a simple model to capture the strongly rising rate seen at several hundred percent

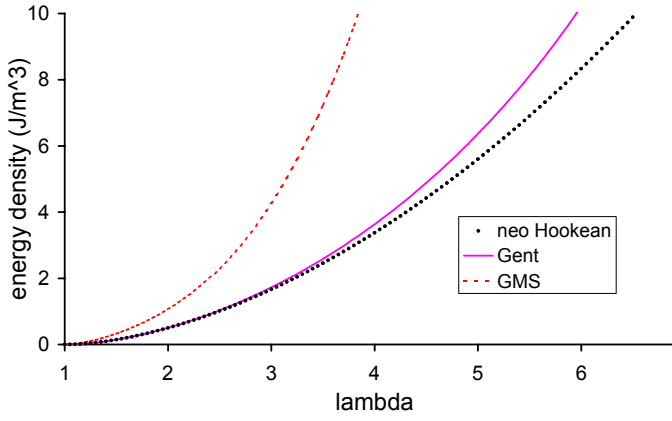


Figure 5. Comparison of the material models in Equations 10, 12 and 13.

strain as the long chain molecules approach their finite extensibility limit:

$$W = -\frac{G}{2}(I_m - 3) \ln \left\{ \frac{I_m - \bar{I}_1}{I_m - 3} \right\} \quad (12)$$

The values used here were $G = 0.5\text{MPa}$ for the shear modulus and $I_m = 100$ for the limiting value for the first strain invariant, corresponding to a maximum possible extension ratio of 9.99.

3.2.3 GMS model

Gregory, Muhr and Stephens (1997) published a model capturing the very high stiffness of filled rubber for small strains:

$$W = \frac{A}{2-n} (\bar{I}_1 - 3 + c^2)^{(2-n)/2} + \frac{B}{2+m} (\bar{I}_1 - 3 + c^2)^{(2+m)/2} + \text{const} \quad (13)$$

where values of $n=0.3$, $A=0.85\text{MPa}$, $m = 1.9$, $B=0.17\text{MPa}$ and $c=0.1$ were used for the material parameters and const is chosen such that $W=0$ at $\bar{I}_1=3$. These values represent a natural rubber compound with 45 parts by weight of reinforcing carbon black (Gough et al. 1999).

3.2.4 Comparison of the models

The predictions of the models are compared for simple extension in Figures 5 and 6.

3.3 Model runs

2-D analyses, whether using full or reduced integration 8-noded elements, were all able to run to 500% strain without any convergence problems. 3-D analyses had difficulty running to 500% strain due to excessive distortion. The problem was solved by using 8 noded

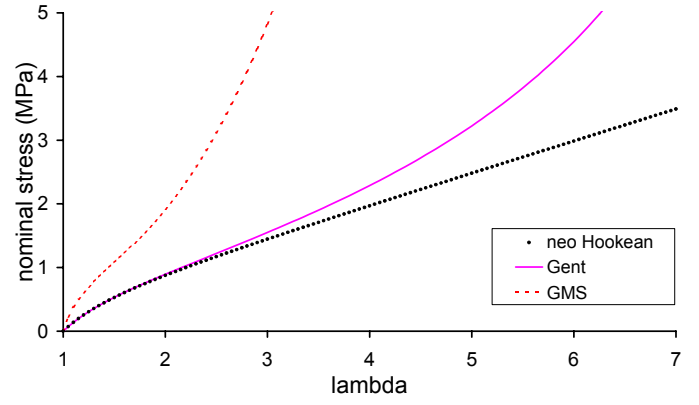


Figure 6. Tensile stress-extension ratio predictions for the models of Equations 10, 12 and 13.

elements, coarse crack blocks (St19x1.sup and St23x1.sup), and reduced integration hybrid elements. The 8 node reduced integration elements were able to analyse FEMs up to 500% strain as opposed to 150% with the 8 noded full integration elements. For detailed information through the thickness, st111x5.sup crack blocks were used.

3.4 Method of determining k

The definition used in Section 2.2 for k was $(U_0 - U_c)/(Wc^2t)$. However, Zencrack uses the J-Integral method to calculate T directly, rather than first calculating U for different crack lengths, so Equation 6 was used to provide an alternative definition:

$$k = \frac{T}{2Wc} \quad (14)$$

for the FE analyses. W is obtained from the element output for an uncracked sheet using the Element strain energy, divided by the element volume, for the entire top row of elements. It was confirmed that this gives the same answer as insertion of the far field extension ratio into the strain energy function to within 4%, provided $c < 0.2w$.

For the 3-D analyses, Zencrack reports the energy release rate as a function of y , based on the J-integral routine of ABAQUS. An averaged value of k may then be defined by the equation:

$$k_{ave} = \frac{1}{t} \int_{y=-t/2}^{y=t/2} k dy \quad (15)$$

Composite Simpson's rule was used to evaluate this integral.

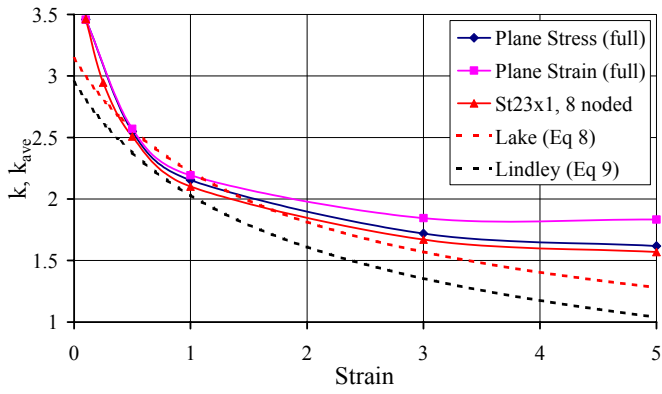


Figure 7. Comparison of k values from 2-D and 3-D analyses (neo-Hookean material) with Equations 8 and 9.

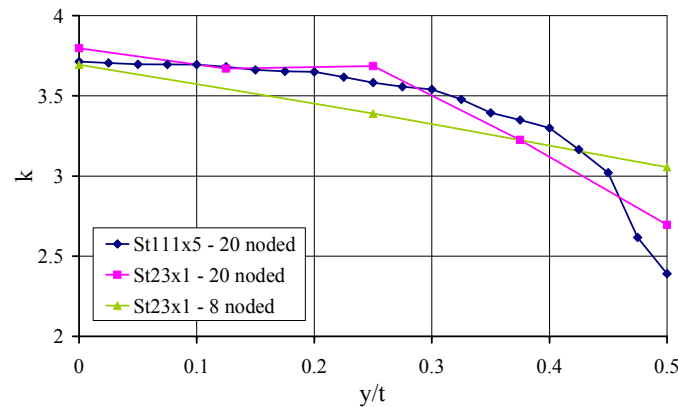


Figure 8. Variation of k through the thickness, $c = 3\text{mm}$ and $t = 2\text{mm}$, (neo-Hookean material, for 10% strain)

3.5 Results

3.5.1 Effect of strain

Figure 7 compares neo-Hookean 2-D and 3-D models with Equations 8 and 9. The 2-D plane stress FEM agrees well with the 3-D FEM and agreement with the equations is good in the strain range typical of experimental characterization (25 to 100% strain). At small strains the FEA results predict a higher value of k than the equations, as could be expected from the correction to Equation 7 for an edge crack, giving a small strain value for k of 3.93. The full integration plane strain results give somewhat higher values for k at strains greater than 100%. The reduced integration plane strain and plane stress results (not shown in the Figure) were very close to the full integration plane stress results.

3.5.2 Effect of rubber thickness

The 3-D analyses predict that T , and hence k as calculated from Equation 14, is a function of distance y from the sheet centre (Figure 8). For larger strains there is less difference between centreline or edge values of k , and the difference is negligible for strains higher than 100%. Typically for 3-D analysis (Ander-

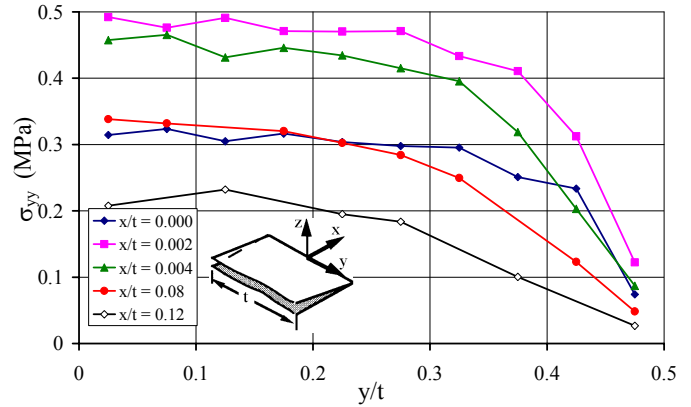


Figure 9. σ_{yy} ahead of crack front ($c = 2.5\text{mm}$) for a sheet of thickness 0.5mm (neo-Hookean material, 10% strain)

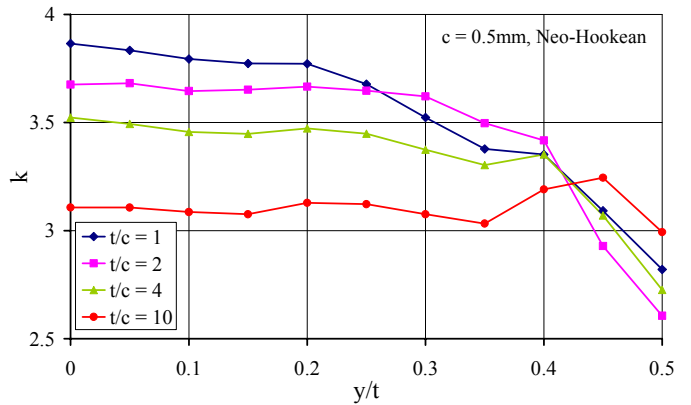


Figure 10. k through the thickness for different sheet thicknesses (neo-Hookean material, 10% strain)

son 1995), plain strain occurs at the centre of the sheet ($y/t = 0$), and plane stress occurs at the edge ($y/t = 0.5$), consistent with Figure 9. The effect of sheet thickness on k is shown in Figure 10 for a crack size of 0.5mm . At the edge of the sheet k is smaller than at the centre, which indicates plane stress at the edge and plane strain at the centre. For the thickest sheet, k depends little on y and the average value is depressed below the plane stress result. The effect of sheet thickness on k_{ave} is shown in Figure 11 for crack sizes of 0.5mm and 2.5mm . For crack lengths smaller than the sheet thickness, k is dependent on the sheet thickness. The dependence of k on the sheet thickness for crack lengths greater than the sheet thickness is small.

3.5.3 Effect of crack length

FEA results for k_{ave} for 2mm thick SEN specimens with crack lengths from 2 to 13mm are shown in Figure 12. Noting that $w = 25\text{mm}$, it is apparent that even for cracks substantially longer than $0.2w$ the effect on k_{ave} is modest. Equation 4 is tested in Figure 13, and found to be reasonably applicable for all the crack lengths investigated, in the sense that the lines are straight and pass through the origin. In this Figure, U_0

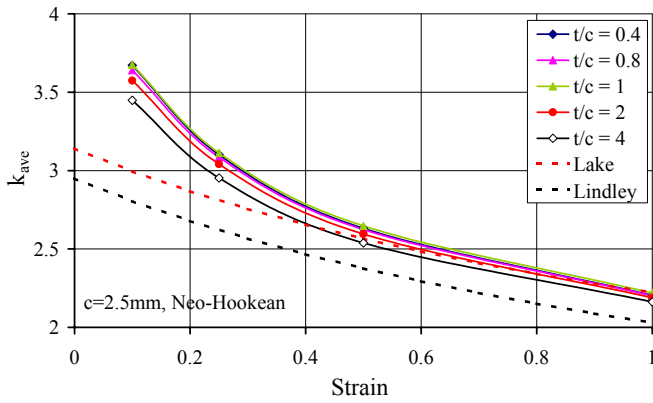


Figure 11. Average k value for different sheet thicknesses as a function of strain

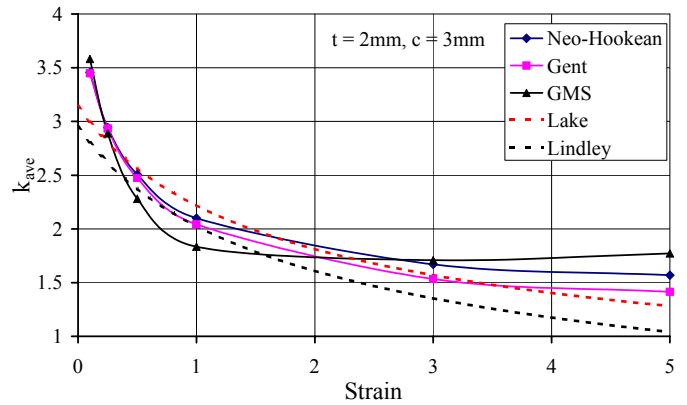


Figure 14. Dependence of k_{ave} on choice of material model

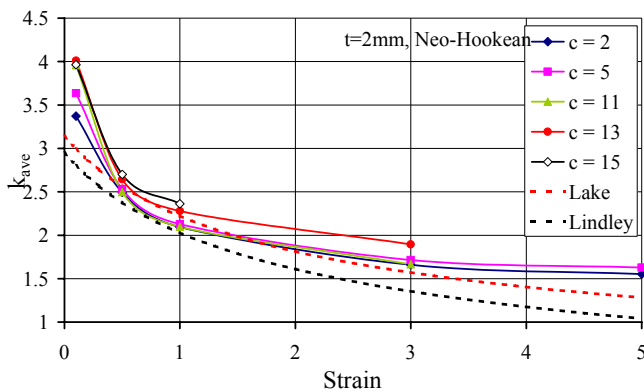


Figure 12 Effect of strain and crack length (for $w = 25\text{mm}$) on k_{ave}

3.5.4 Effect of material model

In addition to the Neo-Hookean model, FEA was also undertaken using the Gent and the GMS models (Figure 14). The different material models give slightly different characteristic k versus strain curves. For large strains the Gent k values are lower than the Neo-Hookean values. The GMS model gives the lowest k values between 25-200% strain of all the three material models, but it results in less decline in k as the strain is increased above 100%, so that at very high strain the GMS model gives the highest k values.

4 INTERNAL CRACKING OF “O” RINGS

“O”ring seals sometimes fail after prolonged stressing in service, even if the application is quasistatic (Stevens 1987). It appears that a crack forms in their interior, driven by the tensile stresses caused by loading. Temperature changes may result in substantial increases in the stress, as a result of thermal expansion of the rubber.

The loading geometry of an unconstrained “O”ring is illustrated in Figure 15; the “O”Ring is flattened between two infinitely stiff flat surfaces.

The dimensions were 46mm length, 49mm diameter reduced by 35% to 31.85mm on compression. A centreline penny shaped crack of initial diameter 0.3mm was inserted in the middle of the specimen, in the vertical plane in which the cylinder axis lies (see Figure 16 in which the crack is not to scale). The 1/8 symmetry FEM, prior to insertion of a crack block, is shown in Figure 17. The crack block used for this problem is shown in Figure 18.

The neo-Hookean material model, with the same values of parameters as in Section 3.2.1, was chosen. Eight noded hydrostatic elements with full integration were used (C3D8H). Results for the strain energy release rate, calculated using the J-integral method, are given in Figure 19.

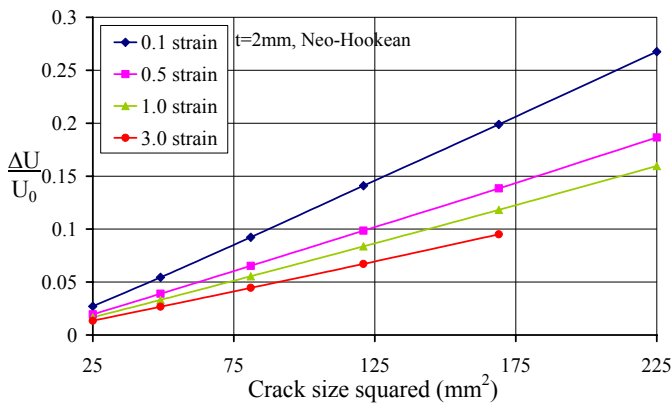


Figure 13 Test of Equation 4

was calculated from the imposed extension ratio by multiplying the calculated strain energy density by the rubber volume. Values of k have been calculated from their gradients, giving 3.71, 2.61, 2.14 and 1.74 for strains of 0.1, 0.5, 1.0 and 3.0 respectively, in good agreement with values calculated from the J-integral method, plotted in Figures 7, 11 and 12. This gives further evidence also of the conservative nature of the criterion $c < 0.2w$, since for all the points plotted in Figure 13 c is equal to or greater than $0.2w$.

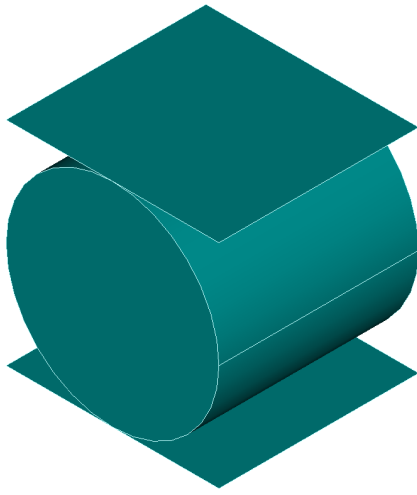


Figure 15 Model O ring prior to loading between two flats

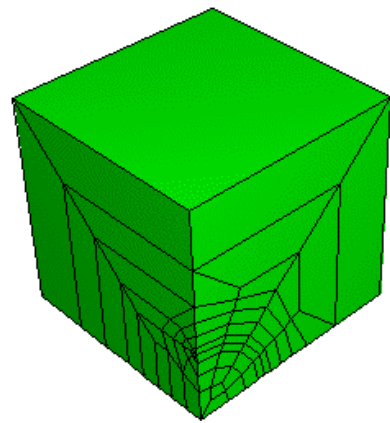


Figure 18. Crack block

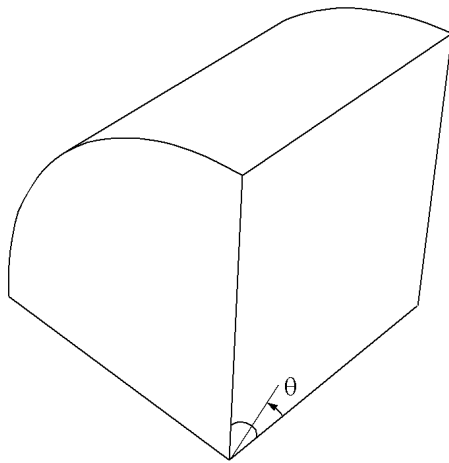


Figure 16 Schematic showing the crack location in the 1/8th geometry

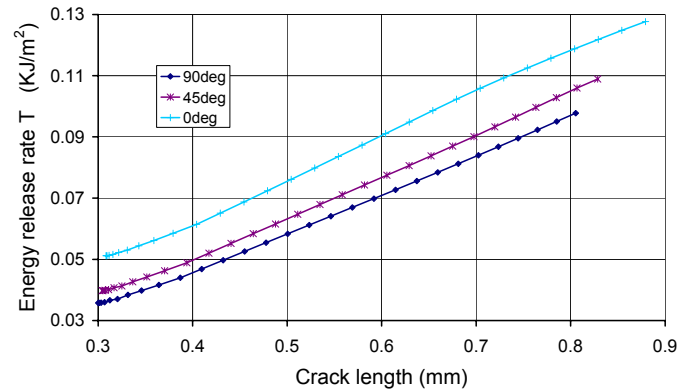


Figure 19. Strain energy release rate as a function of crack length for three values of angle θ ; 0° is the axial direction of the cylinder and 90° is the radial direction.

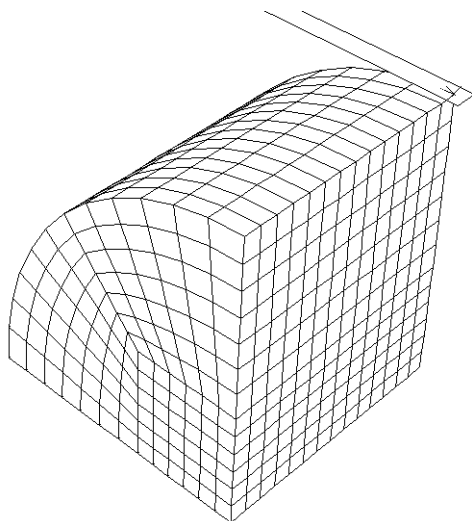


Figure 17 Basic FEM used for O ring; the top surface is compressed in the y direction by a contact plane normal to y

The boundary conditions used in Figure 19 were no slip once contact had been made, and a plane faces at each end of the cylinder. With perfect lubrication at the contact the energy release rate is about 20% lower, and with no stresses applied to the ends the energy release rate falls to less than one third of the values in Figure 19. It is apparent from Figure 19 that an initially circular crack will grow preferentially in the axial direction, becoming elliptical. It is observed experimentally (Stevens 1987) that the crack becomes very much longer in the axial direction than in the radial direction, so that the final stage of failure consists of radial crack growth under conditions of plane strain.

The magnitudes of T given in Figure 19 are very small, noting that below the threshold value T_0 – of the order of 0.05kJm^{-2} for typical elastomers – mechanical crack growth does not occur. This implies that for failure to be a practical problem, the “O”ring would have to be extremely highly compressed, or be made of a material incorporating very large effective flaws, typical effective flaws being less than 0.1mm. However, it should also be borne in mind that “O”rings are usually made from rather hard rubber, with a shear modulus of the order of three times higher than the model used here. This will give an energy release rate, for the same compression displacement, that is three times greater than given in Figure 19.

5 DISCUSSION

It has been found that the numerical results for strain energy release rate of an edge crack in a tensile test piece are reasonably consistent with the result for infinitesimal strain theory ($k = 3.93$), and significantly larger in the small strain limit than suggested by Equations 8 or 9.

For the neo-Hookean model and strains in the range usually employed for determining crack-growth characteristics (25 to 150%), there is good agreement for k values with Equation 8. In conflict with the supposition that k is independent of the strain energy function W , the numerical results for the GMS model fall below Equation 8 and the results of the neo-Hookean and Gent models in this strain range. The problem is presumably a consequence of the very high low-strain stiffness of the GMS model; although this behaviour is typical of elastomers with reinforcing filler, it has been suggested that it is not in fact an elastic effect at all (Ahmadi et al. 2003). The application of fracture mechanics to such materials therefore raises further issues to be resolved than just evaluating k . Thus, Equation 8 remains a useful working approximation for interpreting crack growth data.

Yeoh (1998) and Busfield (2000) also studied the SEN testpiece for rubber using FEA, and reached similar conclusions regarding the accuracy of Equation 8. Yeoh (1998) commented that his results for k were typically a few percent lower than expected, which he ascribed to the relatively coarse mesh density used. Busfield (2000) also found that his results for k for very short cracks were too small for the same reason, and suggested that several elements are needed along the length of the crack to ensure accurate results. The refined mesh at the crack tip provided by Zencrack crack blocks should ensure good accuracy.

The 3D nature of the strain-energy release rate calculations of Zencrack opens up the possibility of simulating the non-uniform rate of propagation across the crack front. According to Figures 8 and 10, the energy release rate is greatest in the interior, so it is predicted that an initially straight crack front will tend to become curved as it propagates, with the fracture in the center of the sheet being in advance of that on the surface.

For the crack in the "O" ring the capability of Zencrack to calculate the local energy release rate around the crack front is invaluable. Previous FE analyses of cracking of "O" rings have used plane strain, and can only deal with the later stages of crack growth once the crack has become long in the axial direction (Medri & Strozzi 1986, Stevens 1987).

To predict service life, it is necessary to obtain accurate energy release rates for small flaws (typically in the range 0.02 to 0.1mm), and to see how crack growth propagates from such flaws. The ability to model the

evolution of a penny-shaped crack, for example, into a new shape that may propagate in a way that is life-limiting or stabilise, is also required. Zencrack provides a suitable tool to these ends. Experimental characterisation of the material for effective flaw size and for crack growth rate would of course also be needed (Gent et al. 1964).

6 CONCLUSIONS

The usual expression for energy release rate in a rubber SEN test piece has been confirmed to be adequate for characterisation purposes, although it underestimates the energy release rate at strains significantly less than 50% strain and significantly greater than 150%.

The work has established that Zencrack, using the J-integral in ABAQUS, has a good capability of calculating energy release rates for cracks in 3D elastomeric bodies with finite strains. It has the ability to simulate crack growth, by automatically propagating the mesh (taking into account experimental characteristics, and allowing the crack front to become curved) and resubmitting the mesh to the FE solver.

REFERENCES

- Ahmadi, H.R., Kingston, J.G.R., Muhr, A.H., Gracia, A. & Gomez, B. 2003. Interpretation of high low-strain modulus of filled rubbers as an inelastic effect. In J.J.C. Busfield & A.H. Muhr (eds) *Constitutive Models for Rubbers III* Rotterdam: Balkema
- Anderson, T.L. 1995. *Fracture Mechanics, Fundamentals and Applications*, second edition, section 2.9
- Busfield, J.J.C. 2000. The prediction of the mechanical performance of elastomeric components using FEA *PhD thesis* London: Queen Mary.
- Busfield, J.J.C., Thomas, A.G. & Ngah, M.F. 1999. Application of fracture mechanics for the fatigue life prediction of carbon black filled elastomers. In A. Dorfmann & A.H. Muhr (eds) *Constitutive Models for Rubber* Rotterdam: Balkema
- Chang, S.J. 1972 Path independent integral for rupture of perfectly elastic materials. *Z. Angew. Math. Phys.* 23: 149-152
- Ewalds, H.L. & Wainhill, R.J.H. 1984 *Fracture Mechanics*. Arnold, Delft.
- Gent, A. N. 1996 A new constitutive equation for rubber. *Rubber Chemistry & Technology* 69: 59-61
- Gent, A. N, Lindey, P.B. & Thomas, A.G. 1964 Cut growth and fatigue of rubbers. I The relationship between cut growth and fatigue. *J. Applied Polymer Science* 8: 455-466
- Gough, J., Gregory, I.H. & Muhr, A.H. 1999 Determination of constitutive equations for vulcanized rubber. In D. Boast & V.A. Coveney (eds), *Finite Element Analysis of Elastomers*: 5-26 London: Professional Engineering Publications.
- Greensmith, H.W. 1963. Rupture of rubber. X: The change in stored energy on making a small cut in a test piece held in simple extension. *J. Applied Polymer Science* 7: 993-1002
- Gregory, I.H., Muhr, A.H. & Stephens, I. J. 1997 Engineering applications of rubber in simple extension. *Plastics, rubber and Composites Processing and Applications* 26: 118-122.

- Lake, G.J. 1970 Application of fracture mechanics to failure in rubber articles, with particular reference to tyres. *Proc. Int Conference on Yield, Deformation and Fracture of Polymers, Cambridge UK*
- Lake, G.J & Lindley, P.B. 1964 Ozone cracking, flex cracking and fatigue of rubber. *Rubber Journal* 146: 24-36.
- Lindley, P.B. 1972 Energy for crack growth in model rubber components. *J. Strain Analysis* 7: 132-140
- Rice, J.R. 1968 A path independent integral and the approximate analysis of strain concentration by notches and cracks. *J. Applied Mathematics* 35: 379-386
- Rivlin, R.N. & Thomas, A.G. 1953 Rupture of rubber I Characteristic energy for tearing. *J Polymer Science* 10(3): 291-318
- Stevens, C.A. 1987 Prediction of fracture in unconstrained elastomeric O-ring Seals *Fluid Sealing Conference, Brighton*
- Thomas, A.G. 1955 Rupture of rubber. II The strain concentration at an incision. *J. Polymer Science* 18: 177-188
- Timoshenko, S. 1934 *Theory of Elasticity* McGraw-Hill, New York.
- Yeoh, O.H. 1998 Strain energy release rates for some classical rubber test pieces by FEA. *Paper 2, Fall meeting of ACS Rubber Division, Nashville*. To appear in V.A. Coveney (ed) *Lifetime prediction of rubber components*, London.